

Electronic Supplementary Information (ESI) for

**KF·B(OH)₃: a KBBF-type material with large birefringence and
remarkable deep-ultraviolet transparency**

Yang Li,^a Xinglong Chen^b and Kang Min Ok^{*a}

^a*Department of Chemistry, Sogang University, 35 Baekbeom-ro, Mapo-gu, Seoul 04107, Korea*

^b*Materials Science Division, Argonne National Laboratory, Lemont, Illinois 60439, United States*

*E-mail: kmok@sogang.ac.kr

Experimental section

Crystal growth

KHF₂ (Sigma, 99 %) and H₃BO₃ (Daejung, 99.5 %) were used as received to grow the KF·B(OH)₃. KHF₂ (5.0 g) and H₃BO₃ (1.5 g) were dissolved in 12.5 mL of distilled water in a plastic dish. The sticky samples were slowly evaporated at room temperature. The block crystals were grown for several weeks in a 60% yield based on H₃BO₃. Although crystals of KF·B(OH)₃ are water-soluble, the material slowly decomposes in water. In addition, KF·B(OH)₃ is moisture-sensitive in a humid condition at room temperature.

Powder X-ray diffraction

The PXRD data of KF·B(OH)₃ were collected via the Mini Flex 600 diffractometer using a Cu K α ($\lambda = 1.54406 \text{ \AA}$) radiation with 40 kV and 15 mA at room temperature. The sample was scanned in the 2θ range of 5-70° at a scan speed of 20°/min and a scan step width of 0.02°. The measured diffraction pattern of the title compound matched well with the stimulated one (**Fig. S4**).

Single-crystal X-ray diffraction

The crystal structure of KF·B(OH)₃ was determined via a Bruker D8 QUEST diffractometer with Mo K α radiation source ($\lambda = 0.71073 \text{ \AA}$) at Sogang University at room temperature. SAINT and SADABS programs were used for data reduction and absorption correction. OLEX2 package was used to solve and refine the structure.¹⁻³ The program PLATON was applied to validate if there is any missing higher symmetry.⁴ Crystallographic data, structure refinement information, atomic coordinates, equivalent isotropic displacement parameters, bond valence sums of all atoms except for H atoms, selected bond lengths, bond angles, and hydrogen bonds were listed in the ESI (**Tab. S1–S6**).

Energy dispersive analysis by X-ray (EDX)

EDX was conducted by a JSM-7100F Thermal field emission electron microscope with lens type ZrO/W Schottky field emission gun. Well-ground solid samples of the title compounds were attached on carbon tape and coated by Pt before the measurements. (**Fig. S5**)

IR spectroscopy

Infrared (IR) spectrum in the range of 500 to 4000 cm⁻¹ were recorded on a Thermo Scientific Nicolet iS50 FT-IR spectrometer. The ground sample was contacted on the diamond attenuated-total-reflectance crystal (**Fig. S6**).

UV-vis-NIR diffuse reflectance spectroscopy

Ultraviolet-visible-near infrared (UV-vis-NIR) diffuse-reflectance spectrum for KF·B(OH)₃ was performed using a Lambda 1050 scan UV-vis-NIR spectrophotometer over the spectral range of 190–900 nm at room temperature. The reflection spectrum was converted to the absorbance data via the Kubelka-Munk function.⁵

Thermal analysis

Thermogravimetric analysis (TGA) was measured via a SCINCO TGA-N 1000 thermal analyzer. The ground polycrystalline sample was loaded into an alumina crucible and heated to 900 °C at a rate of 10 °C min⁻¹ under flowing air. Differential scanning calorimetry data were also obtained on a TA DSC-Q2000 from room temperature to 450 °C at a heating rate of 5 °C min⁻¹ under flowing nitrogen (**Fig. S7**).

Theoretical calculations

The CASTEP package was applied for the first-principles calculations based on density-functional theory.⁶ The band structure, the density of states, and the optical properties were calculated by using the Perdew-Burke-Ernzerhof (PBE) generalized gradient approximation (GGA) and the on-the-fly generated (OTFG) norm-conserving pseudopotential (NCP).⁷⁻¹⁰ Plane-wave cut-off energy of 925 eV was chosen and the dense *k*-point sampling less than 0.03 Å⁻¹ was adopted. The linear optical properties were examined based on the dielectric function $\epsilon(\omega) = \epsilon_1(\omega) + i\epsilon_2(\omega)$. The imaginary part of dielectric function ϵ_2 can be calculated based on the electronic structures and the real part is obtained by the Kramers–Kronig transformation, accordingly the refractive indices and the birefringence (Δn) can be calculated (**Figs. S8-S10**).

Table S1. Crystal data and structure refinement for $\text{KF}\cdot\text{B}(\text{OH})_3$.

Formula	$\text{KF}\cdot\text{B}(\text{OH})_3$
Formula weight	119.93
Temperature/K	297.15
Crystal system	Orthorhombic
Space group	<i>Pbcm</i>
$a/\text{\AA}$	5.4454(3)
$b/\text{\AA}$	10.6284(7)
$c/\text{\AA}$	7.0024(4)
$\alpha/^\circ$	90
$\beta/^\circ$	90
$\gamma/^\circ$	90
Volume/ \AA^3 , Z	405.27(4), 4
$\rho_{\text{calc}}/\text{g/cm}^3$	1.966
μ/mm^{-1}	1.192
$F(000)$	240.0
Crystal size/ mm^3	$0.156 \times 0.147 \times 0.042$
Radiation	Mo-K α ($\lambda = 0.71073$)
2θ range for data collection/ $^\circ$	7.484 to 56.762
Index ranges	$-7 \leq h \leq 7, -14 \leq k \leq 14, -9 \leq l \leq 9$
Reflections collected	15066
Independent reflections	547 [$R_{\text{int}} = 0.0343, R_{\text{sigma}} = 0.0110$]
Data/restraints/parameters	547/0/40
Goodness-of-fit on F^2	1.297
Final R indexes [$I \geq 2\sigma(I)$]	$R_1 = 0.0227, wR_2 = 0.0535$
Final R indexes [all data]	$R_1 = 0.0253, wR_2 = 0.0546$
Largest diff. peak/hole / $e \text{\AA}^{-3}$	0.29/-0.33

^[a] $R_1 = \sum ||F_o| - |F_c|| / \sum |F_o|$ and $wR_2 = [\sum w (F_o^2 - F_c^2)^2 / \sum w F_o^4]^{1/2}$ for $F_o^2 > 2\sigma(F_o^2)$

Table S2. Atomic coordinates ($\times 10^4$), equivalent isotropic displacement parameters ($\text{\AA}^2 \times 10^3$) and bond valence sum calculations for $\text{KF}\cdot\text{B}(\text{OH})_3$. U_{eq} is defined as 1/3 of the trace of the orthogonalized U_{ij} tensor.

Atom	x	y	z	U_{eq}	BVS
K1	6625.1(7)	2500	0	22.97(16)	+1.05
B1	2087(4)	4450.2(19)	2500	19.9(4)	+3.05
O1	4576(2)	4282.5(12)	2500	24.1(3)	-1.33
O2	1208(2)	5653.8(12)	2500	29.4(4)	-1.28
O3	569(2)	3434.3(12)	2500	26.4(3)	-1.25
F1	3277.2(19)	1419.9(10)	2500	29.7(3)	-0.24

Table S3. Bond Lengths for $\text{KF}\cdot\text{B}(\text{OH})_3$.

Atom	Atom	Length/ \AA	Atom	Atom	Length/ \AA
O1	B1	1.367(2)	O2	K1 ⁴	2.8823(11)
O1	K1 ¹	2.8105(10)	O2	K1 ⁵	2.8823(11)
O1	K1	2.8105(10)	F1	K1 ¹	2.7760(9)
O3	B1	1.360(2)	F1	K1	2.7760(9)
O3	K1 ²	2.9434(11)	K1	K1 ¹	3.5012(2)
O3	K1 ³	2.9434(11)	K1	K1 ⁶	3.5012(2)
O2	B1	1.366(2)			

¹+X,+Y,1/2-Z; ²-1+X,+Y,1/2-Z; ³-1+X,+Y,+Z; ⁴1-X,1-Y,1/2+Z; ⁵1-X,1-Y,-Z; ⁶+X,+Y,-1/2-Z

Table S4. Bond Angles for $\text{KF}\cdot\text{B}(\text{OH})_3$.

Atom	Atom	Atom	Angle/ $^\circ$	Atom	Atom	Atom	Angle/ $^\circ$
O3	B1	O1	119.93(17)	F1	K1	O1	67.99(3)
O3	B1	O2	122.05(16)	F1 ⁶	K1	O1	81.56(2)
O2	B1	O1	118.02(16)	F1 ⁶	K1	O1 ⁶	67.99(3)
O1	K1	O1 ⁶	133.21(5)	F1	K1	O1 ⁶	81.56(2)
O1 ⁶	K1	O3 ⁷	152.57(4)	F1 ⁶	K1	O3 ⁷	135.62(3)
O1	K1	O3 ⁸	152.57(4)	F1 ⁶	K1	O3 ⁸	104.10(2)
O1 ⁶	K1	O3 ⁸	72.05(3)	F1	K1	O3 ⁸	135.62(3)
O1	K1	O3 ⁷	72.05(3)	F1	K1	O3 ⁷	104.10(2)
O1 ⁶	K1	O2 ⁹	94.70(3)	F1	K1	O2 ⁹	66.69(3)
O2 ⁹	K1	O3 ⁸	80.37(3)	F1 ⁶	K1	O2 ⁴	66.69(3)
O2 ⁹	K1	O3 ⁷	64.51(3)	F1	K1	O2 ⁴	158.98(3)
O2 ⁴	K1	O3 ⁸	64.51(3)	F1 ⁶	K1	O2 ⁹	158.98(3)
O2 ⁴	K1	O3 ⁷	80.37(3)	F1 ⁶	K1	F1	97.90(4)
O2 ⁴	K1	O2 ⁹	131.66(5)				

¹+X,+Y,1/2-Z; ²-1+X,+Y,1/2-Z; ³-1+X,+Y,+Z; ⁴1-X,1-Y,-Z; ⁵1-X,1-Y,1/2+Z; ⁶+X,1/2-Y,-Z; ⁷1+X,+Y,+Z; ⁸1+X,1/2-Y,-Z; ⁹1-X,-1/2+Y,+Z; ¹⁰+X,+Y,-1/2-Z

Table S5. Hydrogen Bonds for KF·B(OH)₃.

D	H	A	$d(\text{D-H})/\text{\AA}$	$d(\text{H-A})/\text{\AA}$	$d(\text{D-A})/\text{\AA}$	D-H-A/ $^\circ$
O1	H1	F1 ¹	0.81	1.74	2.5550(16)	178.2
O3	H3	F1	0.74	1.86	2.5996(17)	180.0
O2	H2	F1 ²	0.78	1.80	2.5744(17)	169.3

¹1-X,1/2+Y,1/2-Z; ²-X,1/2+Y,1/2-Z³+X,+Y,1/2-Z; ⁴-1+X,+Y,+Z; ⁵-1+X,+Y,1/2-Z; ⁶1-X,1-Y,1/2+Z; ⁷1-X,1-Y,-Z**Table S6.** Hydrogen Atom Coordinates ($\text{\AA}\times 10^4$) and Isotropic Displacement Parameters ($\text{\AA}^2\times 10^3$) for KF·B(OH)₃.

Atom	x	y	z	U_{eq}
H1	5288.66	4955.97	2500	49(8)
H3	1336.61	2863.02	2500	48(9)
H2	-196.87	5793.46	2500	54(9)

Table S7. Comparisons of the Interlayer Bonding for K₂Be₂BO₃F (KBBF) and KF·B(OH)₃ (KFBOH).

Species	Atom1	Atom2	Bonds lengths (\AA)	q_1^a	q_2^a	F
KFBOH	K1	O1	2.81	+1	-2	0.253
		O1	2.811	+1	-2	0.253
		O3	2.943	+1	-2	0.231
		O3	2.943	+1	-2	0.231
		O2	2.882	+1	-2	0.241
		O2	2.882	+1	-2	0.241
		F1	2.776	+1	-1	0.130
		F1	2.776	+1	-1	0.130
Total						1.709
KBBF	K1	F1	2.756	+1	-1	0.132
		F1	2.756	+1	-1	0.132
		F1	2.756	+1	-1	0.132
		F1	2.756	+1	-1	0.132
		F1	2.756	+1	-1	0.132
		F1	2.756	+1	-1	0.132
Total						0.790

^a In multiples of 1.602×10^{-19} C. Cations and anions are regarded as ideal point charges with respective expected valence states.

Table S8. Properties of reported [B(OH)₃]-containing Cocrystal.

Compounds	λ_{cutoff} (nm)	BOH Groups	Band Gap (eV) (HSE06)	Δn	SHG (\times KDP)	Refs.
Cs ₃ [B(OH) ₃] ₂ Cl ₃	180	[B(OH) ₃]	6.31	0.057@ 532 nm	-	11
CsB ₃ O ₃ (OH) ₃ Cl	<200	[B ₃ O ₃ (OH) ₃]	6.40	0.109@ 532 nm	-	11
Cs[B(OH) ₃][B ₃ O ₃ (OH) ₃]Cl		[B ₃ O ₃ (OH) ₃] & [B(OH) ₃]	6.49	0.123@ 532 nm	-	11
Rb ₃ [B(OH) ₃][B ₃ O ₃ (OH) ₃] ₂ Cl ₃		[B ₃ O ₃ (OH) ₃] & [B(OH) ₃]	6.49	0.120@ 532 nm	-	11
Na(COOH)[B(OH) ₃](H ₂ O) ₂		[B(OH) ₃]	Unreported	Unreported	-	12
K ₃ (COOH) ₃ [B(OH) ₃] ₂		[B(OH) ₃]			-	12
(HCOOH) ₃ [B(OH) ₃] ₂ ·3H ₂ O		[B(OH) ₃]			0.7	12
Rb ₃ (COOH) ₃ [B(OH) ₃] ₂		[B(OH) ₃]			0.09 @ 1064 nm	-
Cs ₃ (COOH) ₃ [B(OH) ₃] ₂	[B(OH) ₃]	0.10 @ 1064 nm	-	13		
(NH ₄) ₃ [B(OH) ₃] ₂ (COOH) ₃	[B(OH) ₃]	0.156 @ 546 nm	0.6	14		
KF·B(OH) ₃	<190	[B(OH) ₃]	7.63	0.117@ 532 nm	-	This work

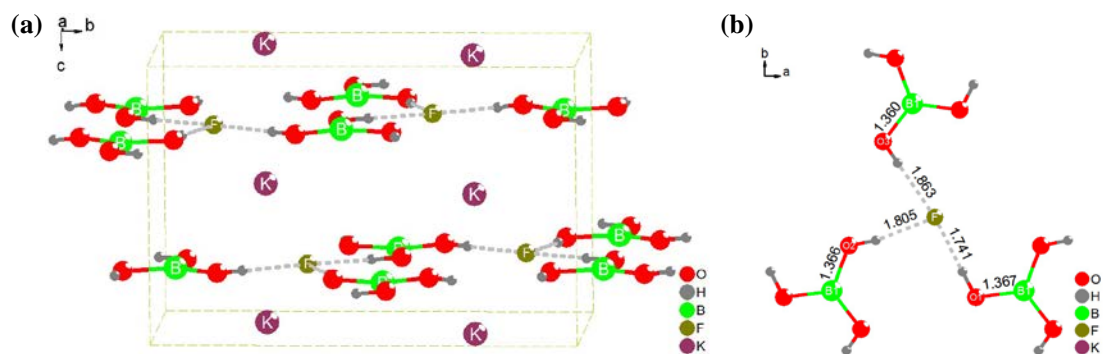


Fig. S1 (a) Structures of $\text{KF} \cdot \text{B}(\text{OH})_3$. $\text{K}-\text{F}$ and $\text{K}-\text{O}$ bonds were omitted to show the layer clearly; (b) Hydrogen bonds between F^- and $[\text{B}(\text{OH})_3]$.

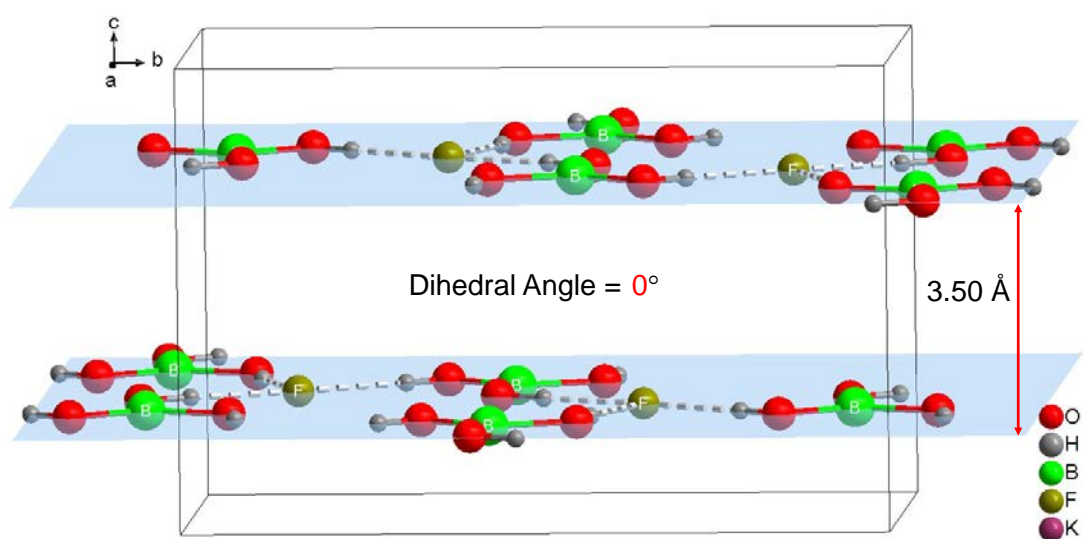


Fig. S2 Distance and dihedral angle between adjacent $[\text{F} \cdot \text{B}(\text{OH})_3]^-$ layers in $\text{KF} \cdot \text{B}(\text{OH})_3$.

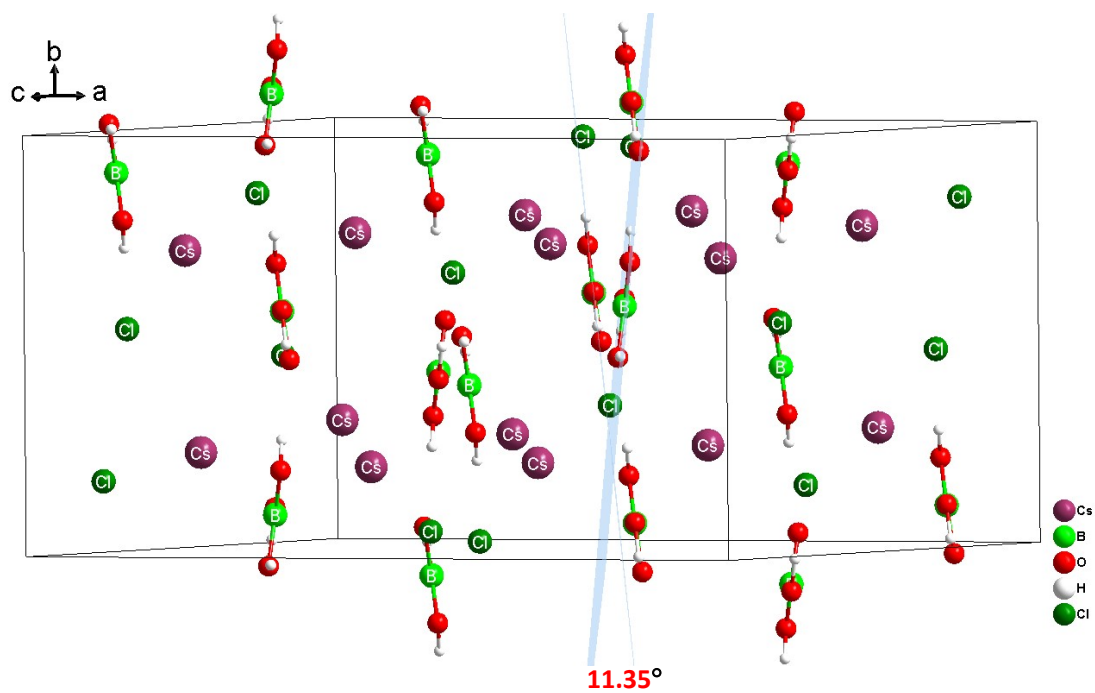


Fig. S3 The dihedral angle of $[B(OH)_3]$ in $Cs_3[B(OH)_3]_2Cl_3$.

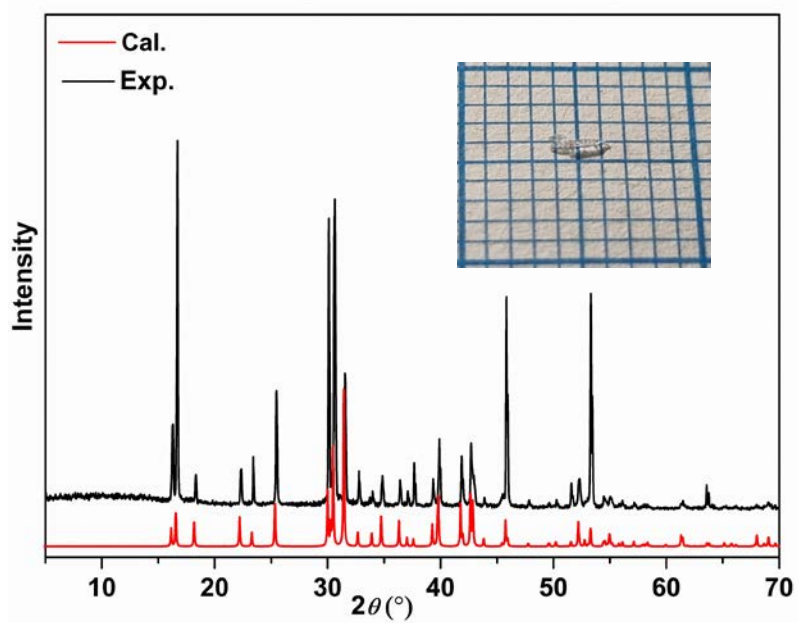
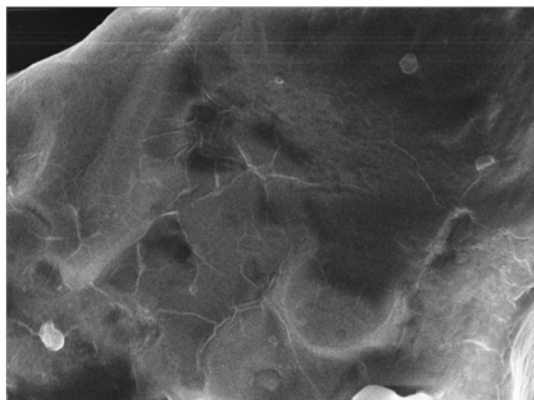
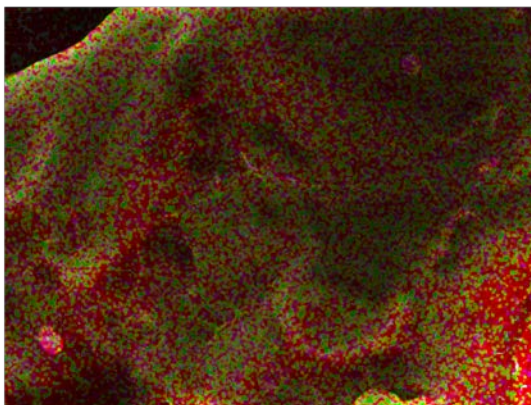


Fig. S4 Experimental and calculated PXRD patterns for $KF \cdot B(OH)_3$. Inset: the photo of an as-grown crystal of $KF \cdot B(OH)_3$. Each division represents 1 mm.

Electron Image 4

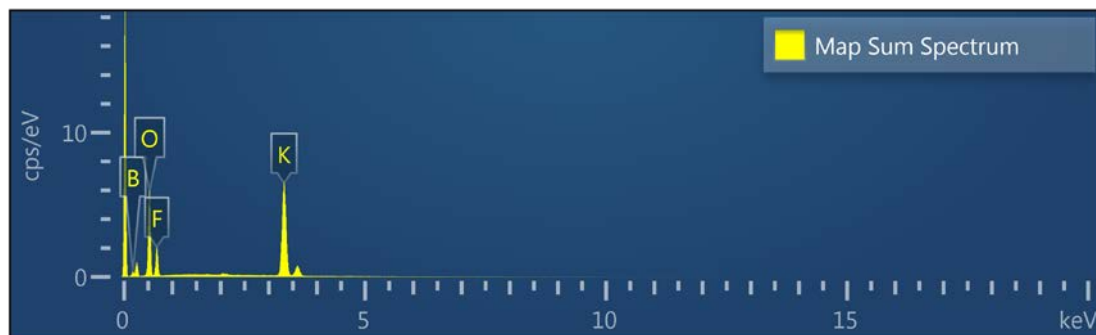


EDS Layered Image 4

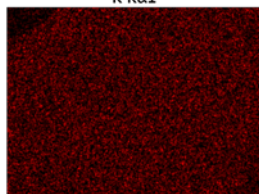


10μm

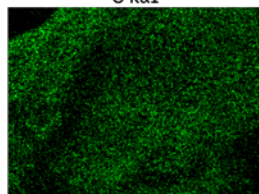
10μm



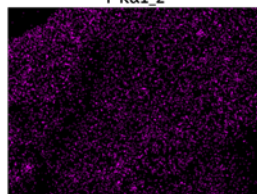
K Kα1



O Kα1



F Kα1_2



B Kα1_2

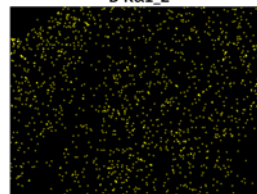


Fig. S5 SEM-EDX spectra for $\text{KF}\cdot\text{B}(\text{OH})_3$.

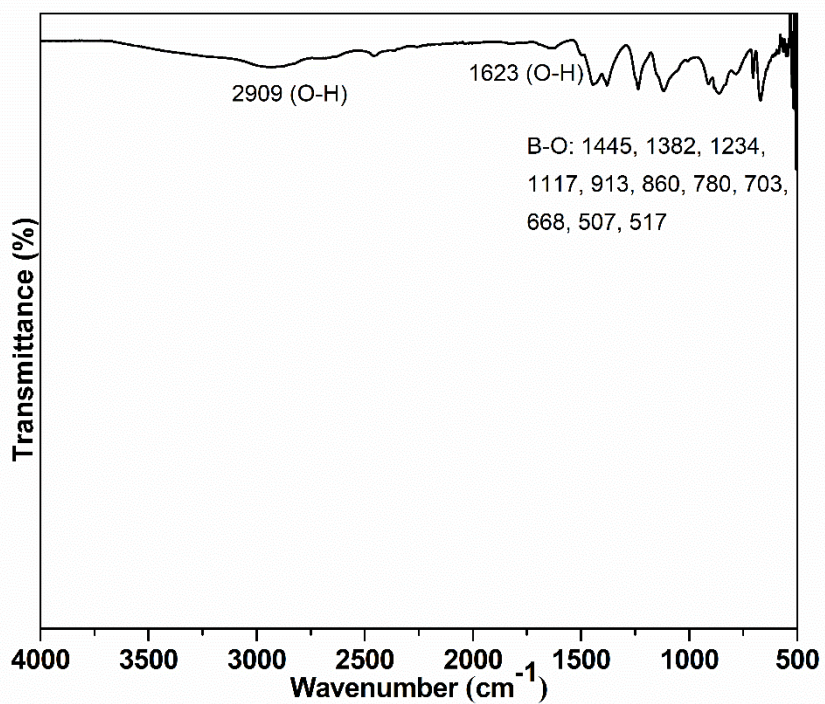


Fig. S6 IR spectrum of KF·B(OH)₃.

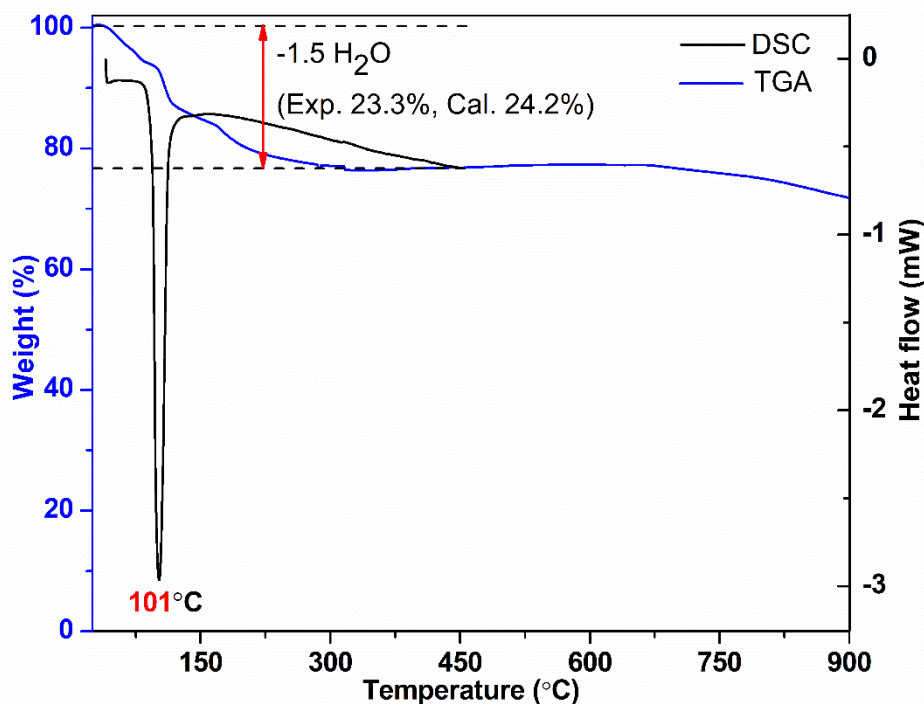


Fig. S7 TGA and DSC diagrams of $\text{KF}\cdot\text{B}(\text{OH})_3$.

The first weight loss in the TGA diagram should be attributed to the decomposition of $\text{B}(\text{OH})_3$ to release water molecules (observed, 22.5%; calculated 24.2%). Similar decomposition process has been observed before from other $\text{B}(\text{OH})_3$ -containing crystals (*Angew. Chem. Int. Ed.* **2022**, *61*, e2022050.). Also, to find an accurate decomposition temperature, we measured the differential scanning calorimetry (DSC) data for $\text{KF}\cdot\text{B}(\text{OH})_3$. As seen in the DSC curve, the decomposition temperature is ca. 100 °C.

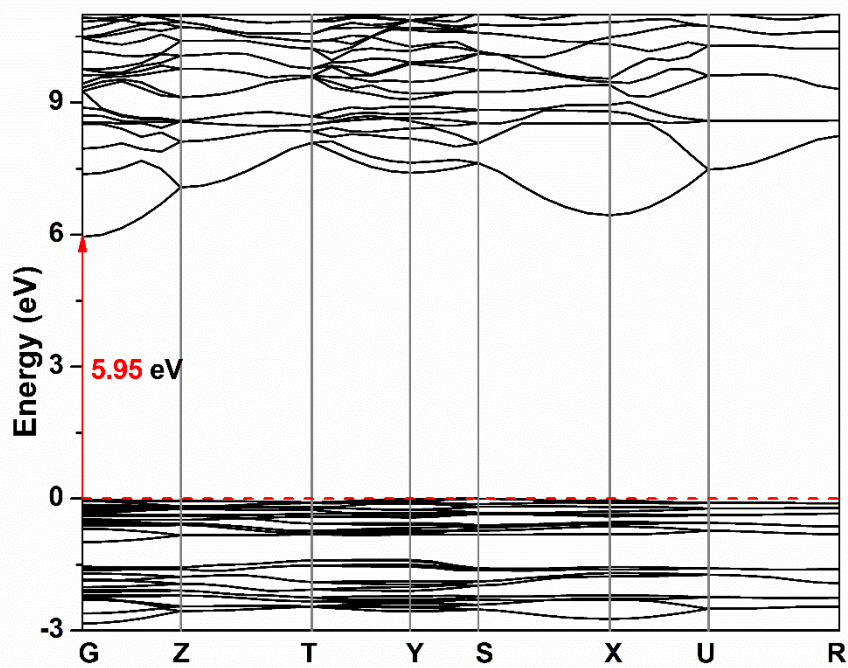


Fig. S8 Band structure of $\text{KF}\cdot\text{B}(\text{OH})_3$.

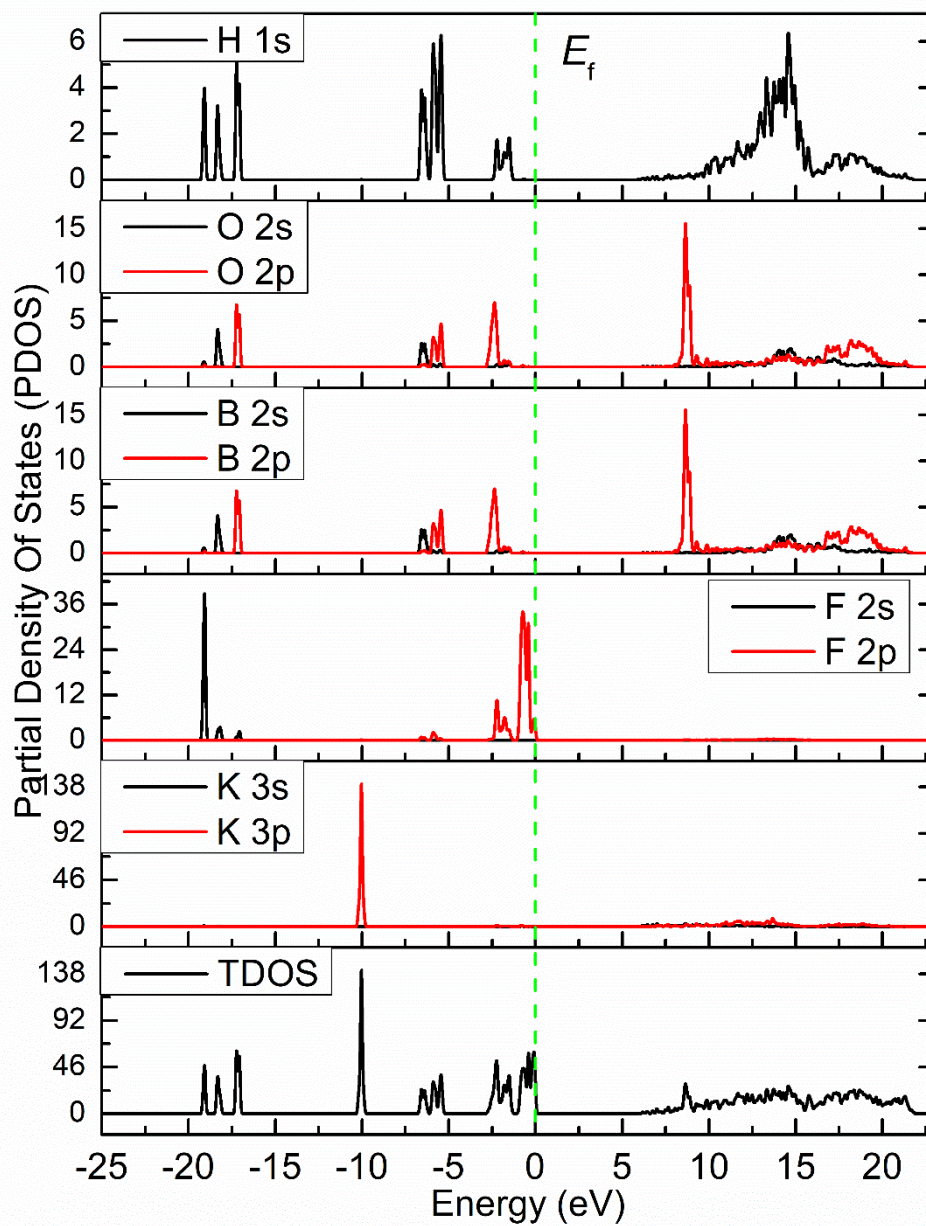


Fig. S9 Density of states for $\text{KF} \cdot \text{B}(\text{OH})_3$.

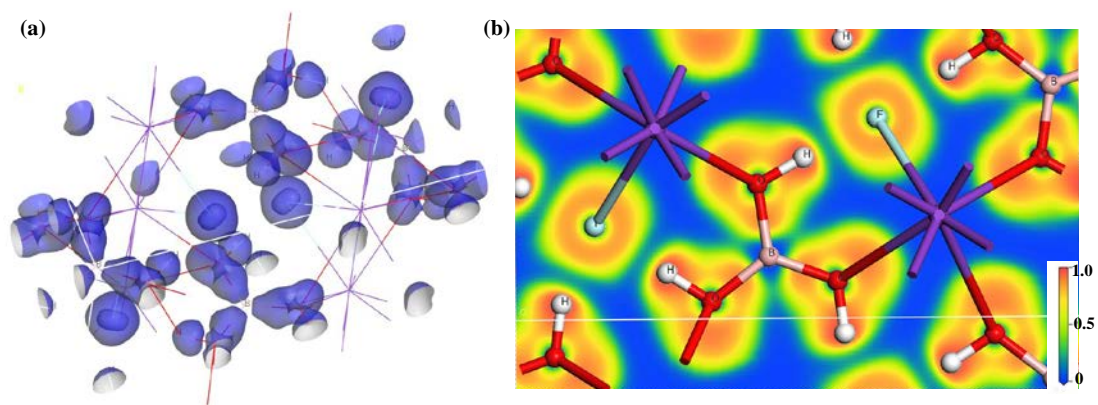


Fig. S10 (a) Electron difference density and (b) Electron localization function diagram of $\text{KF} \cdot \text{B}(\text{OH})_3$.

References

1. Saint, version 7.60A Bruker Analytical X-Ray Instruments, Inc., Madison, WI, 2008.
2. Bruker Suite, Bruker AXS Inc., Madison, USA, 2008.
3. V. Dolomanov, L. J. Bourhis, R. J. Gildea, J. A. K. Howard and H. Puschmann, *J. Appl. Crystallogr.*, 2009, **42**, 339–341.
4. L. Spek, *Acta Crystallogr. Sect. D.*, 2009, **65**, 148–155.
5. J. Tauc, *Mater. Res. Bull.*, 1970, **5**, 721–729.
6. S. J. Clark, M. D. Segall, C. J. Pickard, P. J. Hasnip, M. I. J. Probert, K. Refson and M. C. Payne, *Zeitschrift fur Krist.*, 2005, **220**, 567–570.
7. W. Wang, H. Fan and Y. Ye, *Polymer (Guildf)*, 2010, **51**, 3575–3581.
8. J. P. Perdew, K. Burke and M. Ernzerhof, *Phys. Rev. Lett.*, 1996, **77**, 3865–3868.
9. K. Liu, H. Fan, P. Ren and C. Yang, *J. Alloys Compd.*, 2011, **509**, 1901–1905.
10. J. S. Lin, A. Qteish, M. C. Payne and V. Heine, *Phys. Rev. B: Condens. Matter Mater. Phys.*, 1993, **47**, 4174.
11. J. H. Jiao, M. Cheng, R. Yang, Y. C. Yan, M. Zhang, F. F. Zhang, Z. H. Yang and S. L. Pan, *Angew. Chemie Int. Ed.*, DOI:10.1002/anie.202205060.
12. F. F. He, Q. Wang, M. J. Liu, L. Huang, D. J. Gao, J. Bi and G. H. Zou, *Cryst. Growth Des.*, 2018, **18**, 4756–4765.
13. Y. Q. Guo, D. Zhang, T. Zheng, L. Huang, D. J. Gao, J. Bi and G. H. Zou, *Cryst. Growth Des.*, 2021, **21**, 5976–5982.
14. Y. L. Deng, L. Wang, Y. W. Ge, L. Huang, D. J. Gao, J. Bi and G. H. Zou, *Chem. Commun.*, 2020, **56**, 9982–9985.